Received: 4 October 2016 | Accepted: 18 October 2016

DOI 10.1002/aoc.3685

WILEY Applied Organometallic Chemistry

FULL PAPER

Synthesis, characterization and anticancer activity of a series of curcuminoids and their half-sandwich ruthenium(II) complexes

Peiyuan Li[1] | Wei Su[2,3] | Xiaolin Lei[2] | Qi Xiao[2] | Shan Huang[2]

[1] College of Pharmacy, Guangxi University of Chinese Medicine, Nanning, China

[2] Key Laboratory of Environment Change and Resources Use in Beibu Gulf (Guangxi Teachers Education University), Ministry of Education, China

[3] Department of Chemistry, Guangxi Teachers Education University, Nanning, China

Correspondence
Wei Su, Key Laboratory of Environment Change and Resources Use in Beibu Gulf (Guangxi Teachers Education University), Ministry of Education, China; Department of Chemistry, Guangxi Teachers Education University, Nanning, China.
Email: suwmail@163.com

Funding information
Guangxi Colleges and Universities Key Laboratory of Synthetic; Guangxi Natural Science Foundation, Grant/Award Number: 2016GXNSFCA380013, 2014GXNSFBA118243; National Natural Science Foundation of China, Grant/Award Number: 51263002, 21261005; Natural Functional Molecular Chemistry and Guangxi Teachers Education University; State Key Laboratory for Chemistry and Molecular Engineering of Medicinal Resources; Guangxi Normal University, Grant/Award Number: CMEMR 2016-B16.

A series of curcuminoids (L^1–L^7) and their corresponding (η^6-*p*-cymene)Ru^{II}(Cur)Cl complexes (**1**–**7**) were synthesized and characterized using ^{1}H NMR spectroscopy, elemental analysis and high-resolution electrospray ionization mass spectrometry. The molecular structures of L^2, L^4, **1** and **4** were determined using single-crystal X-ray diffraction analysis. The stability of **1**–**7** was investigated by monitoring their UV profiles. The compounds were further evaluated for their *in vitro* antiproliferative activities against the HepG2 human liver and HeLa human cervical cancer cell lines and HEK-293 T noncancerous cell line.

KEYWORDS

anticancer activity, arene, curcuminoids, ruthenium

1 | INTRODUCTION

Curcumin, 1,7-bis(4-hydroxy-3-methoxyphenyl)-1,6-heptadien-3,5-dione, is the primary bioactive compound isolated from turmeric.[1] Curcumin has a wide spectrum of pharmacological effects including antioxidant, anti-inflammatory, antiviral, antimicrobial and antiproliferative activities.[2] In spite of its promising biological effects, the therapeutic applications of curcumin are restricted because of its low aqueous solubility, slow dissolution rate, instability and poor bioavailability.[3] To address these issues and to improve the systemic bioavailability of curcumin, numerous strategies have been developed, including the use of adjuvants, liposomal curcumin and the design of curcumin derivatives, the so-called curcuminoids.[4] Moreover, curcumin and its analogues can bind to transition metal ions and form metal-based complexes, which offer a promising opportunity for improving the stability and tuning the biological properties such as anticancer activity. The vanadyl, gallium and indium complexes of curcuminoids have been reported, and some of them have shown cytotoxicity for anticancer applications.[5–8]

Among the transition metals, ruthenium appears to be the most promising candidate, since the redox chemistry of ruthenium is rich and compatible with biological media. In addition, the low overall toxicity of ruthenium allows a high dose of treatment.[9] Ruthenium-based complexes have attracted extensive interest for their potential in cancer treatment.[10] For instance, the Ru(III) complexes [HIm][*trans*-$RuCl_4$(DMSO)(Im)] (NAMI-A) and [ImH][*trans*-$RuCl_4(Im)_2$] (KP1019) have been undergoing clinical evaluation with very promising results.[11] Recently, organometallic ruthenium(II) arene complexes, with a half-sandwich type of structure, have been studied as a new source of anticancer metallodrugs.[12] For instance, ruthenium(II) arene complexes with ethylenediamine as the ligand can bind to DNA and thus lead to cytotoxicity towards cancer cells.[13] In

addition, related complexes that contain the 1,3,5-triaza-7-phosphatricyclo[3.3.1.1]decane (PTA) ligand, e.g. [(η^6-*p*-cymene)Ru^{II}(PTA)Cl_2] (RAPTA-C), have exhibited activity against metastases.[14] Moreover, ruthenium–arene complexes incorporating steroidal,[15] picolinamide[16] or carbohydrate[17] ligands have demonstrated promising pharmacological activities particularly antiproliferative effects, making them viable candidates for further biological study.

Recently, ruthenium(II) arene anticancer complexes containing curcumin ligands have been shown to exhibit exciting cytotoxic profiles against selective human cancer cell lines.[18] Dyson and co-workers have shown that ruthenium(II)–arene PTA-type complexes containing curcumin and bisdemethoxycurcumin display potent and selective anticancer activity.[19] In continuation of our previous exploration of ruthenium(II) arene complexes with curcuminoids,[20] and considering the promising biological effects of curcuminoids, we report here the chemical characterization of a series of half-sandwich-type ruthenium (II) complexes (Scheme 1). Furthermore, we present a comparison of the antiproliferative results of these complexes and the corresponding curcuminoid ligands with various cancer cell types.

2 | EXPERIMENTAL

2.1 | Materials

Ruthenium(III) chloride hydrate, curcumin (L^7) and other reagents were purchased from J&K Chemical Co. (China). All reagents and solvents were of high purity and used without further purification. The starting material [(η^6-*p*-cymene)$RuCl_2$]$_2$ was prepared according to previously reported procedures.[20]

2.2 | General procedure for synthesis of curcuminoids

All of the curcuminoid analogues (L^1–L^6) were prepared using literature methods.[21] Aromatic aldehyde (0.01 mol) and tributylborate (4.6 g, 0.02 mol) were dissolved in dry ethyl acetate (0.5 ml). After stirring for 5 min, acetylacetone (0.5 g, 0.05 mol) and boric oxide (0.25 g, 7.5 mmol) were added and, after stirring the reaction mixture, *n*-butylamine (0.4 ml) was added dropwise over a period 30 min. After stirring for 12 h, the reaction mixture was left overnight at room temperature. Dilute hydrochloric acid (0.4 M, 7.5 ml) was added and the mixture was stirred in an oil bath at 60 °C for 1 h. The organic layer was separated after cooling and the aqueous layer was extracted several times with ethyl acetate. The combined organic layer was washed with water, dried over anhydrous $MgSO_4$ and evaporated to yield a gummy product which crystallized from cold methanol. The crude curcuminoid was analyzed using TLC (ethyl acetate–petroleum ether, 1:2) and further purified by flash chromatography using the same eluents.

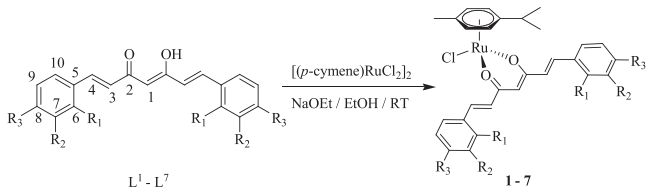

1, L^1: $R_1 = R_2 = R_3 = H$
2, L^2: $R_1 = R_2 = H$, $R_3 = F$
3, L^3: $R_1 = R_2 = H$, $R_3 = OH$
4, L^4: $R_1 = R_2 = H$, $R_3 = OCH_3$
5, L^5: $R_1 = OCH_3$, $R_2 = R_3 = H$
6, L^6: $R_1 = H$, $R_2 = R_3 = OCH_3$
7, L^7: $R_1 = H$, $R_2 = OCH_3$, $R_3 = OH$

SCHEME 1 Curcuminoids and corresponding Ru–arene complexes (L^7: curcumin)

2.3 | Synthesis of complexes

2.3.1 | Complex (η^6-*p*-cymene)Ru(L^1)Cl (1)

[(η^6-*p*-cymene)$RuCl_2$]$_2$ (31.5 mg, 0.05 mmol), L^1 (27.6 mg, 0.1 mmol) and C_2H_5ONa (10.2 mg, 0.15 mmol) were dissolved in 6 ml of ethanol. The reaction mixture was stirred at room temperature. After 1 h, the mixture was dried in vacuum, the residue was redissolved in dichloromethane (10 ml) and the mixture was filtered to remove sodium chloride. Removal of the solvent gave a red solid which was further purified by recrystallization from ethanol and hexane. Yield: 32.8 mg, 60%. HR-ESI-MS (MeOH): *m/z* found (calcd): 511.1212 (511.1219) (100%) [(η^6-*p*-cymene)Ru(L^1)]$^+$. ^{1}H NMR (300 MHz, $CDCl_3$, 25 °C, δ, ppm): 1.31 (d, 6H, J = 6.9 Hz, *p*-cym $CH(CH_3)_2$), 2.37 (s, 3H, *p*-cym CCH_3), 3.00 (m, 1H, *p*-cym $CH(CH_3)_2$), 5.33(d, 2H, J = 6.0 Hz, *p*-cym phenyl-*H*), 5.51 (s, 1H, —C*H*^{1}), 5.60 (d, 2H, J = 6.0 Hz, *p*-cym phenyl-*H*), 6.60 (d, 2H, J = 15.7 Hz, 2× =C*H*$^{3,3'}$), 7.37–7.47 (m, 6H, 4× —Ar*H*$^{7,7',9,9'}$ and 2× —Ar*H*$^{8,8'}$), 7.52–7.55 (m, 4H, 4× —Ar*H*$^{6,6',10,10'}$), 7.64 (d, 2H, J = 15.9 Hz, 2× =C*H*$^{4,4'}$). Anal. Calcd for $C_{29}H_{29}O_2RuCl\cdot{}^3/_4CH_2Cl_2$ (%): C, 58.60; H, 5.04; N, 0. Found (%): C, 58.88; H, 4.83; N, <0.30.

2.3.2 | Complex (η^6-*p*-cymene)Ru(L^2)Cl (2)

This complex was synthesized as for **1**. Yield: 78%. HR-ESI-MS (MeOH): *m/z* found (calcd): 547.1035 (547.1031) (100%) [(η^6-*p*-cymene)Ru(L^2)]$^+$. ^{1}H NMR (300 MHz, $CDCl_3$, 25 °C, δ, ppm): 1.41 (d, 6H, J = 6.9 Hz, *p*-cym $CH(CH_3)_2$), 2.36 (s, 3H, *p*-cym CCH_3), 2.99 (m, 1H, *p*-cym $CH(CH_3)_2$), 5.32 (d, 2H, J = 6.0 Hz, *p*-cym phenyl-*H*), 5.47 (s, 1H, —C*H*^{1}), 5.59 (d, 2H, J = 6.0 Hz, *p*-cym phenyl-*H*), 6.50 (d, 2H, J = 15.7 Hz, 2× =C*H*$^{3,3'}$), 7.04–7.10 (m, 4H, 2× —Ar*H*$^{7,7'}$ and 2× —Ar*H*$^{9,9'}$), 7.48–7.53 (m, 4H, 2× —Ar*H*$^{6,6'}$ and 2× —Ar*H*$^{10,10'}$), 7.58 (d, 2H, J = 15.7 Hz, 2× =C*H*$^{4,4'}$). Anal. Calcd for $C_{31}H_{27}O_2F_2RuCl\cdot{}^3/_4CHCl_3$ (%): C, 54.82; H, 4.02; N, 0. Found (%): C, 54.78; H, 4.23; N, <0.30.

2.3.3 | Complex (η⁶-*p*-cymene)Ru(L³)Cl (3)

See Pettinari *et al.*[19]

2.3.4 | Complex (η⁶-*p*-cymene)Ru(L⁴)Cl (41)

This complex was synthesized as for **1**. Yield: 65%. HR-ESI-MS (MeOH): *m/z* found (calcd): 571.1628 (571.1431) (100%) $[(\eta^6\text{-}p\text{-cymene})Ru(L^4)]^+$. ^{1}H NMR (300 MHz, $CDCl_3$, 25 °C, δ, ppm): 1.41 (d, 6H, J = 6.9 Hz, *p*-cym $CH(CH_3)_2$), 2.36 (s, 3H, *p*-cym CCH_3), 3.01 (m, 1H, *p*-cym $CH(CH_3)_2$), 3.86 (s, 6H, 2× $-OCH_3$), 5.31 (d, 2H, J = 6.0 Hz, *p*-cym phenyl-*H*), 5.45 (s, 1H, $-CH^1$), 5.58 (d, 2H, J = 6.0 Hz, *p*-cym phenyl-*H*), 6.47 (d, 2H, J = 15.7 Hz, 2× $=CH^{3,3'}$), 6.91 (d, 4H, J = 8.8 Hz, 2× $-ArH^{7,7'}$ and 2× $-ArH^{9,9'}$), 7.48 (d, 4H, J = 8.7 Hz, 2× $-ArH^{6,6'}$ and 2× $-ArH^{10,10'}$), 7.59 (d, 2H, J = 15.7 Hz, 2× $=CH^{4,4'}$). Anal. Calcd for $C_{31}H_{33}O_4RuCl\cdot{}^5/_4CH_2Cl_2$: C, 54.38; H, 5.02; N, 0. Found (%): C, 54.54; H, 4.93; N, <0.30.

2.3.5 | Complex (η⁶-*p*-cymene)Ru(L⁵)Cl (5)

This complex was synthesized as for **1**. Yield: 67%. HR-ESI-MS (MeOH): *m/z* found (calcd): 571.1464 (571.1431) (100%) $[(\eta^6\text{-}p\text{-cymene})Ru(L^5)]^+$. ^{1}H NMR (300 MHz, $CDCl_3$, 25 °C, δ, ppm): 1.46 (d, 6H, J = 6.9 Hz, *p*-cym $CH(CH_3)_2$), 2.37 (s, 3H, *p*-cym CCH_3), 3.07 (m, 1H, *p*-cym $CH(CH_3)_2$), 3.92 (s, 6H, 2× $-OCH_3$), 5.31 (d, 2H, J = 6.2 Hz, *p*-cym phenyl-*H*), 5.52 (s, 1H, $-CH^1$), 5.60 (d, 2H, J = 5.9 Hz, *p*-cym phenyl-*H*), 6.67 (d, 2H, J = 15.9 Hz, 2× $=CH^{3,3'}$), 6.91–6.98 (m, 4H, 2× $-ArH^{7,7'}$ and 2× $-ArH^{8,8'}$), 7.33 (m, 2H, 2× $-ArH^{9,9'}$), 7.54 (d, 2H, J = 7.7 Hz, 2× $-ArH^{10,10'}$), 7.98 (d, 2H, J = 15.9 Hz, 2× $=CH^{4,4'}$). ^{13}C NMR (150 MHz, $CDCl_3$, δ, ppm): 17.72 (s, *p*-cym CCH_3), 22.47 (s, *p*-cym $CH(CH_3)_2$), 30.82 (s, *p*-cym $CH(CH_3)_2$), 55.56 (s, OCH_3 of curc), 79.31, 83.12 (s, *p*-cym phenyl-*C*), 97.29 (s, C^1 of curc), 99.49 (s, $C^{3'}$ of curc), 102.21 (s, C^3 of curc), 111.14 (s, $C^{7,7'}$ of curc), 120.72 (s, $C^{9,9'}$ of curc), 124.99 (s, $C^{8,8'}$ of curc), 128.08 (s, $C^{5,5'}$ of curc), 130.34 (s, $C^{10,10'}$ of curc), 133.73 (s, $C^{4,4'}$ of curc), 158.01 (s, $C^{6,6'}$ of curc), 178.86 (s, $C^{2,2'}$ of curc).

2.3.6 | Complex (η⁶-*p*-cymene)Ru(L⁶)Cl (6)

This complex was synthesized as for **1**. Yield: 72%. HR-ESI-MS (MeOH): *m/z* found (calcd): 631.1633 (631.1643) (100%) $[(\eta^6\text{-}p\text{-cymene})Ru(L^6)]^+$. ^{1}H NMR (300 MHz, $CDCl_3$, 25 °C, δ, ppm): 1.38 (d, 6H, J = 6.9 Hz, *p*-cym $CH(CH_3)_2$), 2.35 (s, 3H, *p*-cym CCH_3), 2.98 (m, 1H, *p*-cym $CH(CH_3)_2$), 3.91 (d, 12H, J = 6.8 Hz, 4× $-OCH_3$), 5.30 (d, 2H, J = 5.9 Hz, *p*-cym phenyl-*H*), 5.48 (s, 1H, $-CH^1$), 5.56 (d, 2H, J = 5.9 Hz, *p*-cym phenyl-*H*), 6.46 (d, 2H, J = 15.6 Hz, 2× $=CH^{3,3'}$), 6.85 (d, 2H, J = 6.8 Hz, 2× $-ArH^{9,9'}$), 7.03 (s, 2H, 2× $-ArH^{6,6'}$), 7.08 (m, 2H, J = 7.7 Hz, 2× $-ArH^{10,10'}$), 7.54 (d, 2H, J = 15.6 Hz, 2× $=CH^{4,4'}$). ^{13}C NMR (150 MHz, $CDCl_3$, δ, ppm): 18.11 (s, *p*-cym CCH_3), 22.46 (s, *p*-cym $CH(CH_3)_2$), 30.87 (s, *p*-cym $CH(CH_3)_2$), 55.90, 55.97 (s, OCH_3 of curc), 79.07, 83.04 (s, *p*-cym phenyl-*C*), 97.64 (s, C^1 of curc), 99.55 (s, $C^{3'}$ of curc), 101.88 (s, C^3 of curc), 109.59 (s, $C^{6,6'}$ of curc), 111.16 (s, $C^{9,9'}$ of curc), 121.97 (s, $C^{10,10'}$ of curc), 125.78 (s, $C^{5,5'}$ of curc), 138.53 (s, $C^{4,4'}$ of curc), 149.16 (s, $C^{8,8'}$ of curc), 150.36 (s, $C^{7,7'}$ of curc), 178.38 (s, $C^{2,2'}$ of curc). Anal. Calcd for $C_{33}H_{37}O_6RuCl\cdot{}^5/_4CH_2Cl_2$ (%): C, 53.26; H, 5.16; N, 0. Found (%): C, 53.43; H, 5.30; N, <0.30.

2.3.7 | Complex (η⁶-*p*-cymene)Ru(L⁷)Cl (7)

See Caruso *et al.*[18]

2.4 | Methods and instrumentation

NMR spectra were recorded with a Bruker AV-300 spectrometer at a working frequency of 300 MHz. Chemical shifts (δ) are expressed in parts per million and coupling constants (J) in hertz. Mass spectra for the complexes were recorded with a Waters UPLC XEVO G2 TOF mass spectrometer using an electrospray ionization (ESI) probe. Elemental analyses were carried out using an Elementar Vario EL Cube.

2.5 | X-ray crystallographic determination

All reflection data were collected with a Bruker SMART CCD instrument using graphite monochromatic Mo Kα radiation (λ = 0.71073 Å) at room temperature. A semiempirical absorption correction using the SADABS program was applied, and raw data frame integration was performed with SAINT.[22] The crystal structures were solved by the direct method using the SHELXS-97 program[23] and refined by the full-matrix least-squares method on F^2 for all non-hydrogen atoms using SHELXTL-97[24] with anisotropic thermal parameters. All hydrogen atoms were located in calculated positions and refined isotropically, except the hydrogen atoms of water molecules that were fixed in a difference Fourier map and refined isotropically. The details of the crystal data are summarized in Table 1, and selected bond lengths and angles for L^2, L^4, **1** and **4** are listed in Table 2. Crystallographic data for the structural analysis have been deposited with the Cambridge Crystallographic Data Center, with reference numbers: 1486215 (L^2), 1486216 (L^4), 1486213 (**1**) and 1486214 (**4**).

2.6 | Cell culture and assay for cell viability

HeLa (cervical carcinoma), HepG2 (liver carcinoma) and HEK-293 T human embryonic kidney (a model for healthy cells) cell lines were obtained commercially. Cells were grown in RPMI-1640 supplemented with 10% cosmic calf serum (Hyclone) and antibiotics in a humidified atmosphere of 5% CO_2 at 37 °C. The viability of these cells was determined using the colorimetric Cell Titer 96 aqueous cell proliferation assay (MTT) according to the instructions provided by the manufacturer (Promega, Madison, WI). Briefly, cells (1×10^4–3×10^4 cells per well) were seeded in 96-well plates. One day after seeding, the cells were treated with or without various concentrations of each compound and re-incubated for 72 h. After the

TABLE 1 Crystal data and details of data collection for L^2, L^4, 1 and 4

	L^2	L^4	1	4
Formula	$C_{19}H_{14}F_2O_2$	$C_{21}H_{20}O_4$	$C_{29}H_{29}ClO_2Ru$	$C_{31}H_{33}ClO_4Ru$
M_r	312.30	336.37	546.04	606.09
Crystal system	Monoclinic	Monoclinic	Triclinic	Triclinic
Space group	P21/c	C2/c	P-1	P-1
a (Å)	36.350(5)	11.804(3)	8.2192(17)	7.6052(6)
b (Å)	5.7608(14)	10.836(2)	9.980(2)	11.1063(7)
c (Å)	7.4088(12)	13.835(2)	16.913(3)	17.0498(11)
α (°)	90.00	90.00	96.513(4)	87.248(5)
β (°)	91.308(12)	100.440(19)	102.675(4)	77.073(6)
γ (°)	90.00	90.00	109.297(4)	78.602(6)
V (Å^3)	1551.0(5)	1740.3(6)	1251.1(4)	1375.92(16)
Z	4	4	2	2
D_{calcd} (Mg m^{-3})	1.337	1.284	1.449	1.463
F(000)	648	712	560.0	624
μ (mm^{-1})	0.102	0.088	0.757	0.701
R_{int}	0.0684	0.0781	0.0300	0.0200
θ range (°)	6.72 to 50.04	5.62 to 50.04	4.42 to 50.04	6.1 to 52.74
Reflections collected	7900	5991	17 212	11 641
Independent reflections	2694	1540	4387	5636
GOF (S)	1.082	1.111	1.055	1.045
$R1/wR_2$ [$I \geq 2\sigma(I)$]	0.0561/ 0.1364	0.1085/ 0.3226	0.0239/0.0574	0.0258/0.0654
R_1/wR_2 (all data)	0.0928/ 0.1757	0.1602/ 0.3696	0.0298/0.0600	0.0292/0.0679

cells were washed with sterile phosphate buffer saline, 190 µl of RPMI-1640 and 10 µl of MTT dye solution (5 mg ml^{-1}) were added to each well, and the cells were incubated for an additional 4 h. The medium was discarded; 200 µl of dimethylsulfoxide (DMSO) was added to dissolve the purple formazan crystals formed. The absorbance at 492 nm was measured using a Thermo Scientific Multiskan MK3.

TABLE 2 Selected bond lengths (Å) and angles (°) in L^2, L^4, **1** and **4**

	L^2	L^4	1	4
C2–O1	1.2760(39)	1.2966(69)	1.2815(21)	1.2790(23)
C2′–O1′	1.2902(43)	1.2966(69)	1.2748(21)	1.2759(23)
C3–C4	1.3223(31)	1.3300(75)	1.3158(35)	1.3129(30)
C3–C2	1.4607(38)	1.4326(71)	1.4637(49)	1.4682(27)
C2–C1	1.4015(32)	1.4020(57)	1.3900(32)	1.3920(29)
C1–C2′	1.3838(41)	1.4020(57)	1.3923(31)	1.3914(27)
C2′–C3′	1.4672(36)	1.4326(71)	1.4717(32)	1.4657(28)
C3′–C4′	1.3171(38)	1.3300(75)	1.3221(33)	1.3186(27)
Ru1–centroid			1.6460(3)	1.6514(2)
Ru1–Cl1			2.4179(9)	2.4177(8)
Ru1–O1			2.0678(14)	2.0745(13)
Ru1–O1′			2.0609(16)	2.0579(14)
O1–Ru1–O1′			88.724(60)	89.309(58)
O1–Ru1–Cl1			85.665(52)	85.331(45)
O1′–Ru1–Cl1			84.168(52)	84.369(45)

3 | RESULTS AND DISCUSSION

3.1 | Synthesis and characterization

For the study at hand, a series of curcuminoid ligands (L^1–L^6) were synthesized as reported in the literature.[20] Curcumin (L^7) was purchased commercially. Subsequently, the corresponding half-sandwich (η^6-*p*-cymene)Ru(L)Cl complexes (L = L^1–L^7) were prepared via reaction of each of L^1–L^7 with $[(\eta^6\text{-}p\text{-cymene})RuCl_2]_2$ (Scheme 1). All complexes were characterized using $^1H/^{13}C$ NMR spectroscopy, high-resolution (HR)-ESI-MS and elemental analysis. In addition, crystal structures were obtained for compounds L^2, L^4, **1** and **4**.

The X-ray crystal structures of L^2 and L^4 are shown in Figure 1, with the crystal data being presented in Table 1 and selected bond lengths and angles being presented in Table 2. The structures of L^2 and L^4 are solved in the monoclinic space group P2/c and C2/c, respectively, and the frameworks of both molecules are in a plane. In the structure of L^2, the distances C2—O1 and C2′—O1′ are 1.2760(39) and 1.2902(43) Å, respectively, which are shorter than C—O single bond length (1.43 Å) but longer than double bond length (1.23 Å); and the bond lengths of C1—C2 and C1—C2′ are 1.4015(32) and 1.3838(41) Å, respectively, between C—C single bond length (1.54 Å) and double bond length (1.34 Å), which indicates the enol/keto resonance forms of L^2 (Scheme 2). An intramolecular hydrogen bond between O1 and the proton of O1′ is shown, O1···H—O1′, the length of which is 1.7827(16) Å and the O1···H···O1′ angle is 148.4°. Interestingly, L^4 shows a unique C—C (C1—C2 and

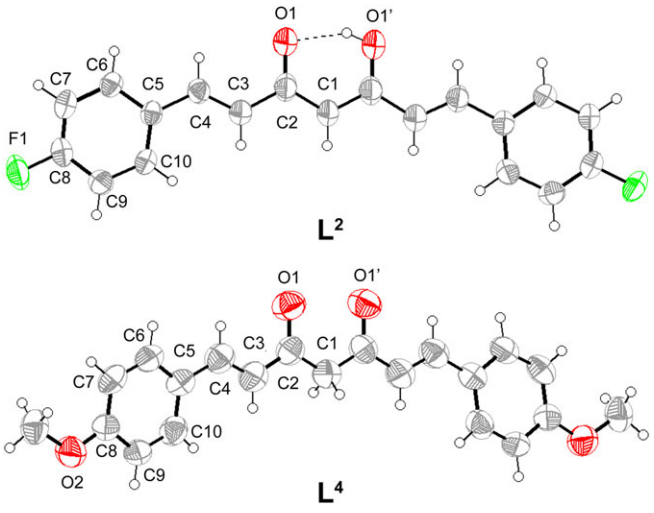

FIGURE 1 ORTEP plots of $L^2$and L^4; thermal ellipsoids are drawn at 50% probability

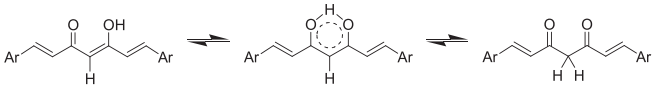

SCHEME 2 Resonance forms of curcuminoids with O1′ protonated

C1—C2′) distance of 1.2966(69) Å, and the whole molecule presents a twofold symmetry that lies on the central carbon atom (C1), which are also described to the enol/keto resonance forms of L^4 (Scheme 2).

Intermolecular hydrogen bonds are formed in the crystal lattices of both L^2 and L^4, and the molecular topology and the presence of hydrogen bonding centers play essential roles in the number of such bonds per molecule. In L^2, the benzene ring (R = C5/C6/C7/C8/C9/C10) and C9′—H proton show intramolecular CH/π interactions with the C9—H proton and the benzene ring (R = C5′/C6′/C7′/C8′/C9′/C10′) of another molecule, distances being 2.8589(4) and 2.8271(4) Å, respectively (Figure 2). In addition, the intermolecular hydrogen bond is found between C7′—H and F1′ of the neighboring molecule (C7′—H···F1′, 2.7283(15) Å). In crystal structure of L^4, the hydrogen bonding interaction is found between two neighboring molecules (C—H···O, 2.6136(40) Å) (Figure 3).

The X-ray crystal structures of **1** and **4** were also determined. Both of them crystallize in the triclinic space group P-1. Their structures are shown in Figure 4, crystallographic data are listed in Table 1 and selected bond lengths and angles are presented in Table 2. In **1** and **4**, Ru(II) adopts the familiar piano-stool geometry with the metal center being coordinated by the *p*-cymene aromatic ring, a terminal chloride and a chelating β-diketone curcuminoid ligand. The distances of Ru–centroid are 1.6460(3) and 1.6514(2) Å, respectively. The Ru—Cl bond lengths are almost equal (*ca* 2.418 Å) and the Ru—O bond lengths vary over a small range (2.0579(14)–2.0745(13) Å). All of the data are in agreement with similar compounds reported elsewhere.[18,20]

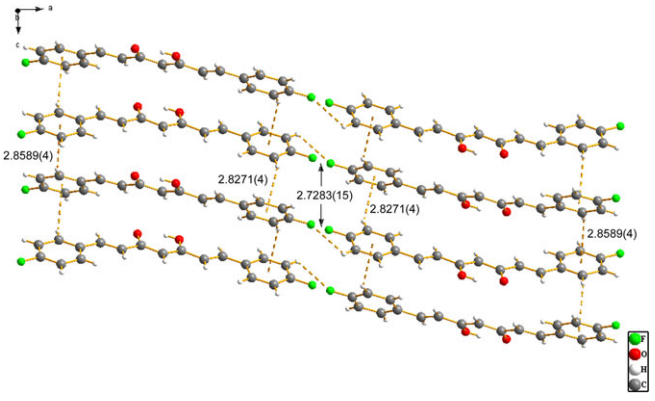

FIGURE 2 Crystal packing of L^2

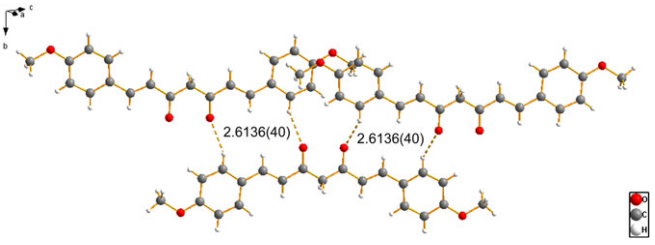

FIGURE 3 Crystal packing of L^4

Different from free ligands, the curcuminoid ligands of **1** and **4** are twisted with torsion angles about the coordination sphere O1–Ru1–O1′–C1′ of 7.960(182)° and 8.063 (168)°, respectively, whereas the angles between the planes of the two phenyl rings in the curcuminoid ligands are 50.328(91)° and 6.781(76)°, respectively (see the profile views of the complexes in Figure 4).

Intermolecular hydrogen bonds are also found in the crystal lattices of **1** and **4**. In the crystal structure of compound **1**, two molecules are interlinked to form a dimer in the unit cell, through a pair of intermolecular hydrogen bonds between N1—H protons and the coordinated chloride ion of another molecule, with a distance of 2.8230(4) Å (Figure 5). Similarly, in compound **4**, dimers are also formed in the unit cell via an intermolecular hydrogen bonding interaction, N1—H···Cl, the length of the hydrogen bond being 3.0369 (2) Å (Figure 6).

3.2 | Stability studies

Since aqueous stability is important factor that affects the bioavailability of Ru–arene complexes,[19,20] the stability of **1–7** was tested by monitoring their UV profiles. The complexes were dissolved in DMSO and followed by water solution, giving a final concentration of 1% (*v*/v) of DMSO. The time-dependent absorption spectra of **1–7** are presented in Figure 7. With absorption being monitored for 72 h, a continued decrease is observed for the

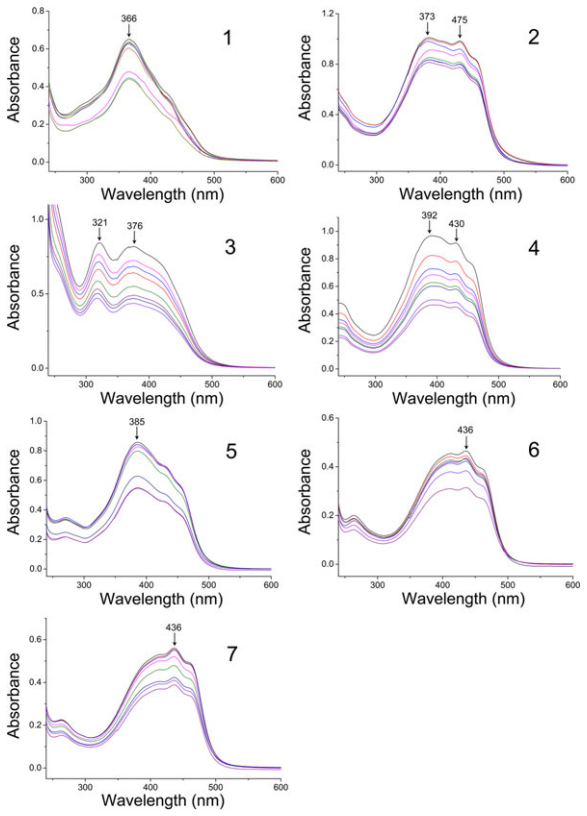

FIGURE 4 Time-dependent UV-visible absorption spectra of **1–7** measured in DMSO–H_2O

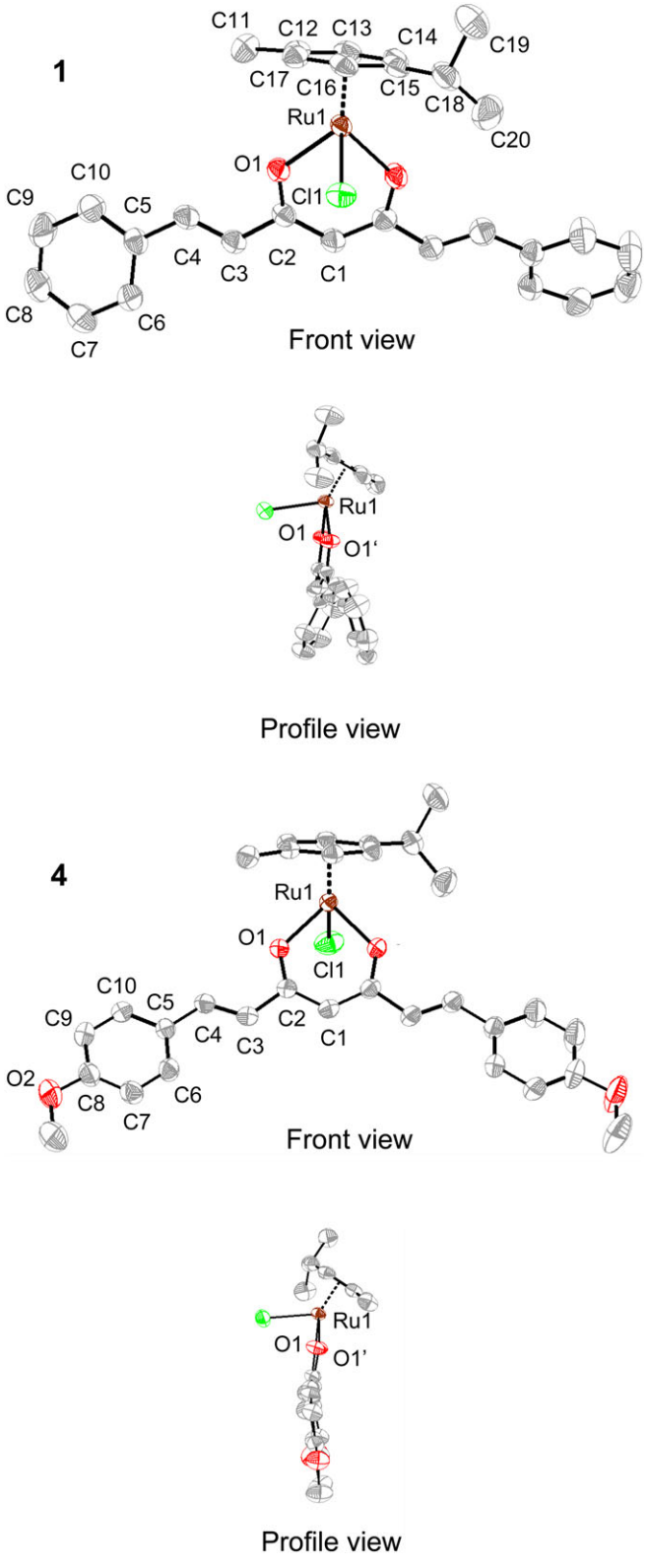

FIGURE 5 ORTEP plots of 1 and 4 (including front view and profile view); thermal ellipsoids are drawn at 50% probability; hydrogen atoms have been omitted for clarity

intensity of the absorption bands of these seven complexes from 366 to 475 nm. This suggests the occurrence of hydrolysis, which is essential in the biological functions of these complexes.[13]

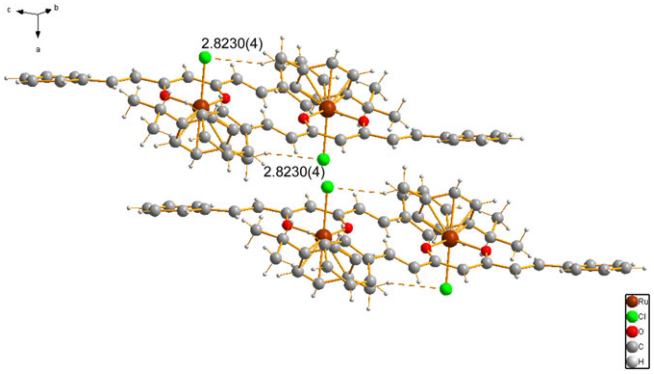

FIGURE 6 Crystal packing of 1

3.3 | Cytotoxicity

The cytotoxicity of the series of curcuminoid ligands L^1–L^7 and their corresponding ruthenium–arene complexes **1–7** was evaluated towards the HepG2 human liver and HeLa human cervical cancer cell lines and HEK-293 T human embryonic kidney (a model for healthy cells) cell line, and for comparison purposes the cytotoxicity of cisplatin was evaluated under the same experimental conditions (Table 3). Most of the curcuminoids are deemed inactive toward these three cell lines (IC_{50} > 100 μM). It is worth noting that curcumin (L^7) shows moderate cytotoxicity against HepG2 with an IC_{50} value of 82.4 μM. Introducing methoxyl groups at the phenolic hydroxyls (L^6) or eliminating the substituent group of the two terminal phenyls (L^1) greatly contributes to the antiproliferative activity in HepG2 cells with IC_{50} values of 15.3 and 12.6 μM, respectively. Most of the ruthenium–arene complexes show moderate micromolar concentrations against cancer cell lines, with IC_{50} values in the 30–79 μM range for HepG2 cell line except **3** and in the 33–65 μM range for HeLa cell line. Towards HEK-293 T cells, comparable IC_{50} values are obtained (19–100 μM), which suggests a lack of cancer cell selectivity. The ruthenium–arene complexes containing curcuminoid ligands have shown moderate activity towards several carcinoma cell lines.[18] Our results show that most of the ruthenium–arene complexes possess higher cytotoxicity in comparison to their free ligands, indicating that the combination of ruthenium–

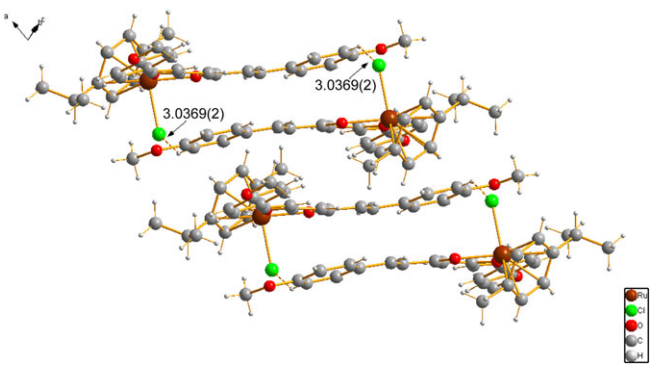

FIGURE 7 Crystal packing of 4

TABLE 3 IC_{50} values (μM) of curcuminoids and corresponding complexes towards HepG2, HeLa and HEK-293 T cell lines

	HepG2	HeLa	HEK-293 T
L^1	15.3 ± 2.1	>100	72.6 ± 8.3
L^2	>100	61.6 ± 0.9	>100
L^3	>100	>100	>100
L^4	>100	>100	>100
L^5	>100	70.2 ± 4.7	>100
L^6	12.6 ± 2.1	>100	>100
L^7	82.4 ± 1.0	51.6 ± 2.0	>100
1	64.5 ± 5.1	35.4 ± 1.2	19.3 ± 1.3
2	74.2 ± 5.0	33.2 ± 0.2	63.3 ± 1.3
3	>100	65.3 ± 3.0	>100
4	52.7 ± 2.6	40.7 ± 1.3	48.2 ± 3.5
5	79.2 ± 3.4	59.1 ± 2.3	>100
6	30.7 ± 0.7	32.6 ± 0.4	42.0 ± 1.5
7	47.0 ± 0.5	52.0 ± 1.2	49.3 ± 0.6
Cisplatin	9.8 ± 0.1	10.0 ± 0.1	11.6 ± 0.3

arene complexes with curcuminoids ligands is an effective strategy for obtaining metallodrugs with promising biological activity. The complexes reported here exhibit antiproliferative activities against the cancer cell lines investigated, and show potential as anticancer drugs.

4 | CONCLUSIONS

Seven curcuminoids (L^1–L^7) and their corresponding ruthenium–arene complexes (**1**–**7**) have been synthesized and characterized using a variety of physical methods. The molecular structures of L^2, L^4, **1** and **4** have been characterized using X-ray crystallography. The *in vitro* activity of all the compounds has been evaluated against the HepG2 human liver and HeLa human cervical cancer cell lines and HEK-293 T healthy cell line. The compounds are moderately cytotoxic towards both human ovarian cancer cells and non-tumorigenic human embryonic kidney cells. Our results indicate that these ruthenium–arene complexes containing curcuminoid ligands have potential for application as anticancer medicines.

ACKNOWLEDGEMENTS

This research was supported by the National Natural Science Foundation of China (21261005, 51263002), Guangxi Natural Science Foundation (2014GXNSFBA118243, 2016GXNSFCA380013), State Key Laboratory for Chemistry and Molecular Engineering of Medicinal Resources (Guangxi Normal University; CMEMR 2016-B16), Guangxi Colleges and Universities Key Laboratory of Synthetic and Natural Functional Molecular Chemistry and Guangxi Teachers Education University. We also thank Prof. Fu-Ping Huang for helpful discussions.

REFERENCES

[1] B. B. Aggarwal, Y. J. Surh, S. Shishodia (Eds), *The Molecular Targets and Therapeutic Uses of Curcumin in Health and Disease*, Springer, New York **2007**.

[2] a) S. H. Wu, L. W. Hang, J. S. Yang, H. Y. Chen, H. Y. Lin, J. H. Chiang, C. C. Lu, J. L. Yang, T. Y. Lai, Y. C. Ko, J. G. Chung, *Anticancer Res.* **2010**, *30*, 2125; b) P. Anand, S. G. Thomas, A. B. Kunnumakkara, C. Sundaram, K. B. Harikumar, B. Sung, S. T. Tharakan, K. Misra, I. K. Priyadarsini, K. N. Rajasekharan, B. B. Aggarwal, *Biochem. Pharmacol.* **2008**, *76*, 1590; c) M. M. Yallapu, M. Jaggi, S. C. Chauhan, *Drug Discovery Today* **2012**, *17*, 71; d) S. V. Jovanovic, C. W. Boone, S. Steenken, M. Trinoga, R. B. Kaskey, *J. Am. Chem. Soc.* **2001**, *123*, 3064; e) J. Barry, M. Fritz, J. R. Brender, P. E. S. Smith, D. K. Lee, A. Ramamoorthy, *J. Am. Chem. Soc.* **2009**, *131*, 4490.

[3] A. O. Boztas, O. Karakuzu, G. Galante, Z. Ugur, F. Kocabas, C. Z. Altuntas, A. O. Yazaydin, *Mol. Pharmaceutics* **2013**, *10*, 2676.

[4] a) P. Anand, A. B. Kunnumakkara, R. A. Newman, B. B. Aggarwal, *Mol. Pharmaceutics* **2007**, *4*, 807; b) X. Qiu, Y. Du, B. Lou, Y. Zuo, W. Shao, Y. Huo, J. Huang, Y. Yu, B. Zhou, J. Du, H. Fu, X. Bu, *J. Med. Chem.* **2010**, *53*, 8260; c) E. Ferrari, F. Pignedoli, C. Imbriano, G. Marverti, V. Basile, E. Venturi, M. Saladini, *J. Med. Chem.* **2011**, *54*, 8066.

[5] a) S. Banerjee, A. R. Chakravarty, *Acc. Chem. Res.* **2015**, *48*, 2075; b) S. Wanninger, V. Lorenz, A. Subhan, F. T. Edelmann, *Chem. Soc. Rev.* **2015**, *44*, 4986.

[6] a) K. Mohammadi, K. H. Thompson, B. O. Patrick, T. Storr, C. Martins, E. Polishchuk, V. G. Yuen, J. H. McNeill, C. Orvig, *J. Inorg. Biochem.* **2005**, *99*, 2217; b) M. Asti, E. Ferrari, S. Croci, G. Atti, S. Rubagotti, M. Iori, P. C. Capponi, A. Zerbini, M. Saladini, A. Versari, *Inorg. Chem.* **2014**, *53*, 4922.

[7] A. Valentini, F. Conforti, A. Crispini, A. D. Martino, R. Condello, C. Stellitano, G. Rotilio, M. Ghedini, G. Federici, S. Bernardini, D. Pucci, *J. Med. Chem.* **2009**, *52*, 484.

[8] N. Aliaga-Alcalde, P. Marqués-Gallego, M. Kraaijkamp, C. Herranz-Lancho, H. den Dulk, H. Görner, O. Roubeau, S. J. Teat, T. Weyhermüller, J. Reedijk, *Inorg. Chem.* **2010**, *49*, 9655.

[9] A. A. Nazarov, C. G. Hartinger, P. J. Dyson, *J. Organomet. Chem.* **2014**, *751*, 251.

[10] a) Y. K. Yan, M. Melchart, A. Habtemariam, P. J. Sadler, *Chem. Commun.* **2005**, 4764; b) A. C. G. Hotze, B. M. Kariuki, M. J. Hannon, *Angew. Chem.* **2006**, *118*, 4957; c) V. Vajpayee, Y. J. Yang, S. C. Kang, H. Kim, I. S. Kim, M. Wang, P. J. Stang, K.-W. Chi, *Chem. Commun.* **2011**, *47*, 5184.

[11] a) J. M. Rademaker-Lakhai, D. Van Den Bongard, D. Pluim, J. H. Beijnen, J. H. M. Schellens, *Clin. Cancer Res.* **2004**, *10*, 3717; b) C. G. Hartinger, M. A. Jakupec, S. Zorbas-Seifried, M. Groessl, A. Egger, W. Berger, H. Zorbas, P. J. Dyson, B. K. Keppler, *Chem. Biodiversity* **2008**, *5*, 2140.

[12] a) C. G. Hartinger, P. J. Dyson, *Chem. Soc. Rev.* **2009**, *38*, 391; b) A. Kurzwernhart, W. Kandioller, S. Bächler, C. Bartel, S. Martic, M. Buczkowska, G. Mühlgassner, M. A. Jakupec, H.-B. Kraatz, P. J. Bednarski, V. B. Arion, D. Marko, B. K. Keppler, C. G. Hartinger, *J. Med. Chem.* **2012**, *55*, 10512; c) A. L. Noffke, A. Habtemariam, A. M. Pizarro, P. J. Sadler, *Chem. Commun.* **2012**, *48*, 5219.

[13] a) H. Chen, J. A. Parkinson, S. Parsons, R. A. Coxall, R. O. Gould, P. J. Sadler, *J. Am. Chem. Soc.* **2002**, *124*, 3064; b) H.-K. Liu, F. Wang, J. A. Parkinson, J. Bella, P. J. Sadler, *Chem. – Eur. J.* **2006**, *12*, 6151.

[14] a) C. Scolaro, A. Bergamo, L. Brescacin, R. Delfino, M. Cocchietto, G. Laurenczy, T. J. Geldbach, G. Sava, P. J. Dyson, *J. Med. Chem.* **2005**, *48*, 4161; b) S. Chatterjee, S. Kundu, A. Bhattacharyya, C. G. Hartinger, P. J. Dyson, *J. Biol. Inorg. Chem.* **2008**, *13*, 1149.

[15] a) J. Ruiz, V. Rodríguez, N. Cutillas, A. Espinosa, M. J. Hannon, *Inorg. Chem.* **2011**, *50*, 9164; b) J. Ruiz, V. Rodríguez, N. Cutillas, K. G. Samper, M. Capdevila, Ò. Palacios, A. Espinosa, *Dalton Trans.* **2012**, *41*, 12847.

[16] P. Chellan, K. M. Land, A. Shokar, A. Au, S. H. An, D. Taylor, P. J. Smith, K. Chibale, G. S. Smith, *Organometallics* **2013**, *32*, 4793.

[17] M. Böge, C. Fowelin, P. Bednarski, J. Heck, *Organometallics* **2015**, *34*, 1507.

[18] a) F. Caruso, M. Rossi, A. Benson, C. Opazo, D. Freedman, E. Monti, M. B. Gariboldi, J. Shaulky, F. Marchetti, R. Pettinari, C. Pettinari, *J. Med. Chem.* **2012**, *55*, 1072; b) L. Bonfili, R. Pettinari, M. Cuccioloni, V. Cecarini, M. Mozzicafreddo, M. Angeletti, G. Lupidi, F. Marchetti, C. Pettinari, A. M. Eleuteri, *ChemMedChem* **2012**, *7*, 2010; c) F. Caruso, R. Pettinari, M. Rossi, E. Monti, M. B. Gariboldi, F. Marchetti, C. Pettinari, A. Caruso, M. V. Ramani, G. V. Subbaraju, *J. Inorg. Biochem.* **2016**, *162*, 44.

[19] R. Pettinari, F. Marchetti, F. Condello, C. Pettinari, G. Lupidi, R. Scopelliti, S. Mukhopadhyay, T. Riedel, P. J. Dyson, *Organometallics* **2014**, *33*, 3709.

[20] X. Lei, W. Su, P. Li, Q. Xiao, S. Huang, Q. Qian, C. Huang, D. Qin, H. Lan, *Polyhedron* **2014**, *81*, 614.

[21] M. A. Khan, R. El-Khatib, K. D. Rainsford, M. W. Whitehouse, *Bioorg. Chem.* **2012**, *40*, 30.

[22] SAINT, *Software Reference Manual*, Bruker AXS, Madison, WI **1998**.

[23] G. M. Sheldrick, *Acta Crystallogr. A* **1990**, *46*, 467.

[24] G. M. Sheldrick, *SHELXS-97, Program for X-ray crystal structure solution*, University of Göttingen, Germany **1997**.

How to cite this article: Li, P., Su, W., Lei, X., Xiao, Q., and Huang, S. (2016), Synthesis, characterization and anticancer activity of a series of curcuminoids and their half-sandwich ruthenium(II) complexes, *Appl Organometal Chem*, doi: 10.1002/aoc.3685